



HAL
open science

Cenozoic reactivation of the Great Glen Fault, Scotland: additional evidence and possible causes

Eline Le Breton, Peter Robert Cobbold, Alain Zanella

► **To cite this version:**

Eline Le Breton, Peter Robert Cobbold, Alain Zanella. Cenozoic reactivation of the Great Glen Fault, Scotland: additional evidence and possible causes. *Journal of the Geological Society*, 2013, 170 (3), pp.403-410. 10.1144/jgs2012-067 . insu-00836055

HAL Id: insu-00836055

<https://insu.hal.science/insu-00836055>

Submitted on 20 Jun 2013

HAL is a multi-disciplinary open access archive for the deposit and dissemination of scientific research documents, whether they are published or not. The documents may come from teaching and research institutions in France or abroad, or from public or private research centers.

L'archive ouverte pluridisciplinaire **HAL**, est destinée au dépôt et à la diffusion de documents scientifiques de niveau recherche, publiés ou non, émanant des établissements d'enseignement et de recherche français ou étrangers, des laboratoires publics ou privés.

1 **Cenozoic reactivation of the Great Glen Fault, Scotland: Additional Evidence and**
2 **Possible Causes**

3

4 E. Le Breton^{1,2*}, P.R. Cobbold¹, A. Zanella¹

5 ¹ Géosciences Rennes, Université de Rennes 1, CNRS, 263 Avenue du Général Leclerc,
6 35042 Rennes, France

7 ² Now at Department of Earth Sciences, Freie Universität Berlin, Berlin, Germany

8

9 *Corresponding author, E. Le Breton, Department of Earth Sciences, Freie Universität Berlin,
10 Malterserstr. 74-100, 12249 Berlin, Germany. eline.lebreton@fu-berlin.de

11

12

13 **Abstract**

14 The Great Glen Fault (GGF) trends NNE-SSW across northern Scotland. According to
15 previous studies, the GGF developed as a left-lateral strike slip fault during the Caledonian
16 Orogeny (Ordovician to Early Devonian). However, it then reactivated right-laterally in the
17 Tertiary. We discuss additional evidence for this later phase. At Eathie and Shandwick, minor
18 folds and faults in fossiliferous Jurassic marine strata indicate post-depositional right-lateral
19 slip. In Jurassic shale, we have found bedding-parallel calcite veins (‘beef’ and ‘cone-in-
20 cone’) that may provide evidence for overpressure development and maturation of organic
21 matter at significant depth. Thus, the Jurassic strata at Eathie and Shandwick accumulated
22 deeper offshore in the Moray Firth and were subject to Cenozoic exhumation during right-
23 lateral displacement along the GGF, as suggested by previous authors. Differential sea-floor
24 spreading along the North East Atlantic ridge system generated left-lateral transpressional
25 displacements along the Faroe Fracture Zone (FFZ) from the Early Eocene to the Late
26 Oligocene (*c.* 47–26 Ma), a period of uplift and exhumation in Scotland. We suggest that such

27 differential spreading was responsible for reactivation of the GGF. Indeed, left-lateral slip
28 along the FFZ is compatible with right-lateral reactivation of the GGF.

29

30 **Introduction**

31 Scotland lies between the NE Atlantic Ocean to the west and north, and the North Sea
32 to the east (**Figure 1**). The Great Glen Fault (GGF) is a major Caledonian tectonic structure
33 that trends NNE-SSW across all of northern Scotland. This strike-slip fault developed left-
34 laterally during the Caledonian Orogeny, in Ordovician to Early Devonian times (e.g. *Hutton*
35 *& McErlean*, 1991; *Soper et al.*, 1992; *Stewart et al.*, 2000, 2001; *Mendum & Noble*, 2010).
36 However, previous studies of seismic data from the Inner Moray Firth (IMF) Basin, Mesozoic
37 strata onshore NE Scotland and Tertiary dyke-swarms in NW Scotland, all indicate right-
38 lateral reactivation of the GGF during the Cenozoic (e.g. *Holgate*, 1969; *Underhill & Brodie*,
39 1993; *Thomson & Underhill*, 1993; *Thomson & Hillis*, 1995). The exact timing and the causes
40 of this reactivation are still uncertain.

41 *Underhill & Brodie* (1993) showed that the IMF underwent regional uplift during the
42 Cenozoic. This they attributed to reactivation of the GGF. More widely, analyses of sonic
43 velocities, vitrinite reflectance and apatite fission tracks have revealed exhumation and uplift
44 of Scotland during the Cenozoic (e.g. *Underhill & Brodie*, 1993; *Thomson & Underhill*, 1993;
45 *Hillis et al.*, 1994; *Thomson & Hillis*, 1995; *Clift et al.*, 1998; *Jolivet*, 2007; *Holford et al.*,
46 2009, 2010). In the Early Palaeogene, significant uplift occurred. This may have been due to
47 the Iceland Mantle Plume or part of the North Atlantic Igneous Province (NAIP) (e.g. *Brodie*
48 *& White*, 1994; *Clift et al.*, 1998; *Jones et al.*, 2002). However, Cenozoic uplift of Scotland
49 appears to have been episodic from 65 to 60 Ma, 40 to 25 Ma and 15 to 10 Ma (e.g. *Holford*
50 *et al.*, 2009, 2010). *Holford et al.* (2010) suggested that the various episodes of uplift were
51 due to intraplate stress from the Alpine Orogeny and plate reorganisation in the NE Atlantic.

52 *Thomson & Underhill* (1993) and *Thomson & Hillis* (1995) attributed uplift of the IMF to
53 Alpine and NE Atlantic events. More recently, *Le Breton et al.* (2012) have shown that
54 variations in the amount and direction of sea-floor spreading, along and between the ridge
55 systems of the NE Atlantic, generated relative displacements along major oceanic fracture
56 zones, the Faroe-Fracture Zone (FFZ), between the Reykjanes and Aegir ridges, and the Jan
57 Mayen Fracture Zone (JMFZ), between the Aegir and Mohns ridges. *Le Breton et al.* (2012)
58 have suggested that this differential sea-floor spreading was responsible for post-breakup
59 compressional deformation of the NW European continental margin.

60

61 On this basis, the four main possible causes of reactivation of the GGF and Cenozoic
62 uplift of Scotland are: (1) mantle processes around the Iceland Mantle Plume, (2) intra-plate
63 compression from the Alpine Orogeny, (3) ridge push from the NE Atlantic and (4) variation
64 in the amount and rate of sea-floor spreading and plate reorganisation in the NE Atlantic. In
65 this paper, we investigate the fourth hypothesis. To this purpose, we describe some field
66 observations of Jurassic outcrops in NE Scotland and we discuss possible causes and timing
67 of reactivation of the GGF.

68

69 **1. Geological Setting**

70 **1.1 Onshore rocks of Scotland**

71 Rocks in Scotland have formed over a time span of billions of years. Various
72 orogenies have been responsible for a wide variety of rock types (**Figure 1**; *Stone*, 2007). The
73 oldest rocks of Europe (~3 Ga), the Lewisian gneiss, are visible in the Hebrides Islands, NW
74 Scotland, whereas, on the mainland along the NW coast, they lie beneath the Neoproterozoic
75 sedimentary strata of the Torridonian Sandstone (~1 Ga). The Moine Thrust is a major fault
76 that separates the Lewisian gneiss and Torridonian Sandstone, to the west, from

77 Neoproterozoic metamorphic rocks of the Moine Supergroup, to the east. In NE Scotland, the
78 Moine Supergroup lies under the Devonian Old Red Sandstone, famous for its fossil fish
79 (*Miller*, 1851). Further south, from Fort William to Inverness, the GGF separates the Moine
80 Supergroup from the Dalradian Supergroup. The latter mostly consists of Neoproterozoic
81 metamorphic rocks and late-Caledonian magmatic intrusions (Silurian-Devonian). South of
82 the Highland Boundary Fault, the Midland Valley is a rift valley containing mostly Palaeozoic
83 strata. The Moine Thrust, the GGF and the Highland Boundary Fault are major tectonic
84 structures, which developed during the Caledonian Orogeny (Ordovician to Early Devonian),
85 during closure of the Iapetus Ocean and continental collision of Laurentia, Baltica and
86 Avalonia (*Soper et al.*, 1992).

87 Mesozoic strata, mostly Jurassic, crop out along the NW and NE coasts. On the NW
88 coast, they occur at Kilchoan, Lochaline and more widely across the Inner Hebrides; on the
89 NE coast, at the mouth of the IMF and along the Helmsdale Fault (**Figure 1**). At Eathie and
90 Shandwick, minor faults, trending NE-SW along the GGF, put Jurassic strata against Old Red
91 Sandstone or Neoproterozoic basement (*Judd*, 1873; *Holgate*, 1969; *Underhill & Brodie*,
92 1993). From fossil evidence, the strata are Kimmeridgian at Eathie and Bathonian to Middle
93 Oxfordian at Shandwick (*Judd*, 1873; *Sykes*, 1975; *Wright & Cox*, 2001). In the Golspie-
94 Helmsdale area, Triassic to Upper Jurassic strata are more widespread (*Stone*, 2007; *Trewin &*
95 *Hurst*, 2009). The Helmsdale Fault separates them from Neoproterozoic basement or the Late
96 Caledonian Helmsdale Granite, to the west. The Upper Jurassic ‘Boulder Beds’ accumulated
97 in deep water in the footwall of the Helmsdale Fault, at a time when that fault was active
98 (*Roberts*, 1989; *Trewin & Hurst*, 2009).

99 Intense volcanic activity occurred along the NE Atlantic margins, during continental
100 breakup in early Palaeogene time, and resulted in the development of the NAIP (*Saunders et*
101 *al.*, 1997). In NW Scotland, this volcanic event was responsible for the development of large

102 gabbroic intrusive centres (e.g. Isles of Skye and Mull), as well as widespread lava flows and
103 dyke swarms (**Figure 1**). Several authors have suggested that the Iceland Mantle Plume was
104 responsible for this widespread magmatic activity (e.g. *White & McKenzie*, 1989; *Saunders et*
105 *al.*, 1997).

106 During the Plio-Pleistocene, glaciation produced U-shaped valleys, such as the Great
107 Glen, and various firths. After the last glacial maximum (approx. 18 kyr ago), isostatic
108 readjustment produced Quaternary raised beaches. Indeed, the readjustment may still be
109 ongoing (*Firth & Stewart*, 2000).

110

111 **1.2 Offshore rocks of NE Scotland**

112 The Mesozoic IMF Basin is a western arm of the North Sea rift (**Figure 2**, *Evans et*
113 *al.*, 2003; *Underhill*, 1991a). Numerous seismic surveys have provided good insights into the
114 structural development of the IMF and the northeastern end of the GGF (**Figure 2**; *Underhill*
115 *& Brodie*, 1993; *Thomson & Underhill*, 1993; *Thomson & Hills*, 1995). Three major faults
116 shaped the basin: the Wick Fault at its northern edge, the Banff Fault to the south and the
117 Helmsdale Fault to the west (**Figure 2**). During Upper Jurassic rifting, fault blocks formed
118 and tilted (*Underhill*, 1991a). However, from interpretation of seismic data, well cores and
119 outcrop data, the overall structure of the basin was that of a half-graben, the depocentre being
120 proximal to the Helmsdale Fault (*Thomson & Underhill*, 1993).

121 *McQuillin et al.* (1982) suggested that a post-Carboniferous right-lateral displacement
122 of about 8 km along the GGF was a critical factor in the development of the IMF Basin. On
123 the other hand, *Underhill & Brodie* (1993) argued that the GGF was inactive as a strike-slip
124 fault, during phases of extension in the IMF, and that the Helmsdale Fault was then the

125 dominant control on the structure. In contrast, the GGF reactivated in the Tertiary, during
126 regional uplift and basin inversion (*Underhill, 1991a*).

127

128 **1.3 Evidence for Cenozoic reactivation of the GGF**

129 The GGF developed as a left-lateral fault during the Caledonian Orogeny (*Hutton &*
130 *McErlean, 1991; Stewart et al., 2000, 2001*). However, according to previous studies, using
131 seismic data from the IMF Basin and analyses of Mesozoic outcrops and Tertiary dyke
132 swarms, the GGF reactivated right-laterally in the Tertiary (*Holgate, 1969; Underhill &*
133 *Brodie, 1993; Thomson & Underhill, 1993; Thomson & Hillis, 1995*).

134 By analysis of the WNW-trending Permo-Carboniferous dyke swarm of northern
135 Argyll, on the northwestern side of the GGF, *Speight & Mitchell (1979)* inferred a right-
136 lateral displacement of 7-8 km, as well as a considerable downthrow to the SE. Moreover,
137 *Holgate (1969)* deduced 29 km of right-lateral slip along the GGF since the Upper Jurassic,
138 from field observations of Jurassic rocks in Argyll. On the island of Mull, Tertiary dykes are
139 offset right-laterally along the GGF (**Figure 1**; *Thomson & Underhill, 1993*), which is
140 consistent with the previous suggestions of *Holgate (1969)* and *Speight & Mitchell (1979)*.

141 On seismic sections from the IMF Basin, the GGF appears as a ‘flower structure’ and
142 inversion structures are visible in the northwestern corner of the basin, along the Wick Fault
143 (**Figure 2**; *Underhill & Brodie, 1993; Thomson & Underhill, 1993*). From structural studies
144 along the GGF in Easter Ross (**Figure 2**), onshore well data from Tain and seismic data from
145 the IMF Basin, *Underhill & Brodie (1993)* identified folds and faults, trending N-S to NNE-
146 SSW, in Devonian strata adjacent to the GGF. Moreover, they suggested that the Jurassic
147 outcrops in Easter Ross along the GGF (**Figure 2**) may be parts of flower structures that
148 resulted from right-lateral slip along the GGF. In Jurassic strata of the Sutherland Terrace

149 (**Figure 2**), next to the Helmsdale Fault, *Thomson & Underhill* (1993) described open folds,
150 attributing them to opposing senses of slip on the Helmsdale Fault (left-lateral) and the GGF
151 (right-lateral).

152 Estimates of right-lateral displacement on the GGF during the Tertiary are small, from
153 8 km to 29 km, depending on the studies (*Holgate*, 1969; *McQuillin et al.*, 1982; *Rogers et*
154 *al.*, 1989; *Underhill & Brodie*, 1993). The exact timing of reactivation is uncertain. Several
155 authors have suggested that reactivation was contemporaneous with regional uplift of the
156 Scottish Highlands during Palaeocene-Eocene events of NE Atlantic rifting or during Oligo-
157 Miocene (Alpine) tectonics (e.g. *Underhill*, 1991b, *Underhill & Brodie*, 1993; *Thomson &*
158 *Underhill*, 1993; *Thomson & Hillis*, 1995).

159

160 **1.4 Evidence for Cenozoic exhumation**

161 From interpretation of seismic and well data, the IMF underwent exhumation during
162 the Cenozoic and the western side of the North Sea tilted to the east (e.g. *Underhill*, 1991b;
163 *Argent et al.*, 2002). Indeed, Jurassic strata in the IMF are *c.* 500-1500 m shallower than they
164 are in the Viking and Central Graben areas to the east. *Thomson & Underhill* (1993) have
165 estimated about 1 km of uplift in the west, decreasing gradually eastwards, whereas *Thomson*
166 *& Hillis* (1995) inferred that exhumation removed about 1.5 km of basin fill from the IMF
167 and *Hillis et al.* (1994) estimated 1 km of Tertiary erosion throughout the whole IMF.

168 Several authors have suggested that Scotland experienced a major phase of uplift in
169 the early Palaeogene, as a result of igneous underplating or dynamic uplift, associated with
170 the Iceland Mantle Plume and widespread magmatic activity west of Scotland (*White &*
171 *Lovell*, 1997; *Nadin et al.*, 1997; *Clift et al.*, 1998; *Jones et al.*, 2002; *Mackay et al.*, 2005;
172 *Saunders et al.*, 2007; *Persano et al.*, 2007). However, fission track analyses on apatite have

173 revealed that Cenozoic exhumation of Scotland was episodic, at 65-60 Ma, 40-25 Ma and 15-
174 10 Ma (*Holford et al.*, 2009, 2010; *Jolivet*, 2007) and may have continued into Late Neogene
175 time (*Hall & Bishop*, 2002; *Stoker*, 2002). *Holford et al.* (2010) have therefore suggested that
176 regional exhumation of Scotland was due mainly to plate-wide horizontal forces, resulting
177 from Alpine orogeny or NE Atlantic events.

178 Coeval with Cenozoic uplift, widespread compressional folds and reverse faults
179 developed on the NW European continental margin, offshore Scotland, (*Boldreel & Andersen*,
180 1993, 1998; *Brekke*, 2000; *Hitchen*, 2004; *Johnson et al.*, 2005; *Ritchie et al.*, 2003, 2008;
181 *Smallwood*, 2004; *Stoker et al.*, 2005; *Tuitt et al.*, 2010). South of the Faroe Islands, such
182 structures (e.g. the Wyville-Thomson ridge, Ymir ridges (WYTR), Alpin Dome and Judd
183 Anticline) formed from the Middle Eocene to the Early Miocene (*Smallwood*, 2004; *Johnson*
184 *et al.*, 2005; *Ritchie et al.*, 2008; *Tuitt et al.*, 2010). The possible causes of shortening are a
185 subject of ongoing debate: (1) Alpine stress field (e.g. *Boldreel & Andersen*, 1993, 1998), (2)
186 ridge push from the NE Atlantic (e.g. *Boldreel & Andersen*, 1993, 1998), (3) plume-enhanced
187 ridge push (*Lundin & Doré*, 2002), (4) stress associated with the development of the Iceland
188 Plateau (*Doré et al.*, 2008) or (5) differential sea-floor spreading along the NE Atlantic
189 (*Mosar et al.*, 2002; *Le Breton et al.*, 2012).

190 In this paper, we further investigate the structural evidence for Cenozoic right-lateral
191 reactivation of the GGF and we discuss possible causes, such as differential sea-floor
192 spreading along the NE Atlantic.

193

194 **2. Method**

195 Our data are from observations of Jurassic outcrops along both the GGF and the
196 Helmsdale Fault (**Figure 3**). Upper Jurassic outcrops at Eathie (Kimmeridgian) and south of

197 Shandwick (Port-an-Righ, Lower and Middle Oxfordian, and Cadh'-an-Righ, from Bathonian
198 to Middle Oxfordian) are accessible only at low tide. Along the Helmsdale Fault, between
199 Golspie and Helmsdale, Jurassic outcrops are more numerous.

200 The objectives of our fieldwork were to identify, measure and analyse structures
201 within Jurassic strata and the nature of their contact with the Old Red Sandstone or
202 Neoproterozoic/Caledonian basement. We compared our observations with previous studies
203 and with published interpretations of seismic data from the IMF, in order to discuss the timing
204 and possible causes of reactivation of the GGF.

205

206 **3. Results**

207 **3.1 Eathie**

208 The Jurassic outcrops on the coast at Eathie are easily accessible at low tide, via the
209 'Hugh Miller Trail'. The sequence consists of alternating shale (containing Kimmeridgian
210 ammonites) and argillaceous limestone, with some sandstone at the northeastern end of the
211 outcrop. The Upper Jurassic rocks at Eathie are in contact mostly with Neoproterozoic
212 basement, except in the northeastern area, where they are in contact with the Old Red
213 Sandstone (**Figures 4 and 5**). Previous studies, notably a drilling site for coal exploration,
214 indicate that the Jurassic strata abut a fault that trends NNE-SSW (**Figure 4**; *Miller*, 1851;
215 *Judd*, 1873; *Institute of Geological Sciences, Sheet 94*, 1973). This fault is probably an eastern
216 splay of the GGF (e.g. *Underhill & Brodie*, 1993). We did not observe a sharp fault contact,
217 but there is evidence for faulting in the form of fault brecciation between Jurassic strata and
218 Neoproterozoic basement.

219 In the south, the Jurassic strata dip seaward at approx. 40-60°. However towards the
220 NE, the dips vary more strongly (from 10 to 90°) around numerous folds, the axes of which

221 plunge gently and trend from N-S to NE-SW (**Figures 4 and 5**). Moreover, several steep
222 calcite veins, parallel to the GGF, cut the entire Jurassic sequence and their sigmoidal shapes
223 indicate right-lateral slip along the fault (**Figure 5**).

224 In the same general area, *Jonk et al.* (2003) described sills and dykes of injected sand.
225 We found that some of these sills resemble ‘beef’ (bedding-parallel veins of fibrous calcite;
226 see *Rodrigues et al.*, 2009), in the sense that they locally contain fibrous calcite or cone-in-
227 cone structures (**Figure 6**). We note that *Hillier & Cosgrove* (2002) described ‘beef’ and
228 ‘cone-in-cone’, together with sandstone intrusions, at a depth of about 2000 m within Eocene
229 sandstone in the Alba oil field of the Outer Moray Firth, attributing these structures to
230 overpressure. In other sedimentary basins (for example, the Neuquén Basin of Argentina, or
231 the Wessex Basin, UK) ‘beef’ veins provide evidence of overpressure and maturation of
232 organic matter at a depth of several km, in the ‘oil window’, where temperature is high
233 enough (60-120 °C) for maturation of organic matter (*Selley*, 1992; *Rodrigues et al.*, 2009).
234 Similarly, the Jurassic shale at Eathie may have accumulated deeper offshore in the IMF
235 Basin and then have been subject to post-Jurassic exhumation (*Hillis et al.*; 1994). This may
236 have occurred during right-lateral slip along the GGF.

237

238 **3.2 Shandwick**

239 Two outcrops of Jurassic strata are accessible on the coast at low tide, south of
240 Shandwick (**Figure 7**). At Port-an-Righ, the strata are Lower to Middle Oxfordian in age,
241 whereas at Cadh’an-Righ there is a complete section, from Bathonian to Middle Oxfordian
242 (*Sykes*, 1975; *Wright & Cox*, 2001). In both areas the Jurassic strata abut the Old Red
243 Sandstone. As at Eathie, this contact is a NNE-SSW fault zone, an eastern branch of the GGF
244 (e.g. *Judd*, 1873, *Underhill & Brodie*, 1993).

245

246 ***Port-an-Righ***

247 The Jurassic strata at Port-an-Righ dip generally seaward at approx. 14° to 32°
248 (**Figures 7 and 8**). However, from the top of the cliffs, a large fold is visible on the wave-cut
249 platform, next to the GGF. The fold is asymmetric and sigmoidal. At its northeastern end, the
250 fold is broadly cylindrical and the fold axis strikes NE-SW, but at its southeastern end, the
251 axis plunges at 16-20° to the SW. Such folds are typical of right-lateral slip within a
252 multilayer (*Richard et al., 1991*). Further toward the NE, the dip of the bedding varies even
253 more (from 12° to the S, through 28-70° to the W, to 10-23° to the E; **Figure 7**). Throughout
254 the area, steep calcite veins offset the Jurassic strata right-laterally (**Figure 8**). The veins
255 strike at approx. 45° to the GGF. In this area, *Jonk et al. (2003)* described right-lateral faults,
256 trending NE-SW and bearing calcite cement. A fault separates Jurassic from Devonian strata
257 (**Figure 8**; *Jonk et al., 2003*), but we did not observe any striae.

258

259 ***Cadh'-an-Righ***

260 Another Jurassic outcrop is visible at Cadh'-an-Righ (**Figure 7**), although access to it
261 is more difficult. In this area, the Devonian strata dip steeply seaward (at about 80° next to the
262 Jurassic strata), whereas the Jurassic strata dip generally seaward at 44-58° (**Figure 7**). Once
263 again, we found 'beef' in the Jurassic strata, as well as coal (**Figure 9**).

264 At Cadh'-an-Righ there is a clear fault contact between Jurassic and Devonian strata
265 (**Figure 9**). The strike of the fault is parallel to the GGF (approx. N040). We found striae that
266 pitch at approx. 8° to the NE, indicating both right-lateral and reverse slip. Thus if the 'beef'
267 formed at a depth of 1500-2500 m, close to the oil window where temperature is high enough
268 for maturation of organic matter (*Rodrigues et al., 2009*), its exhumation would imply a
269 right-lateral displacement along the GGF of approx. 10-18 km. This magnitude is consistent

270 with previous estimates (e.g. *Holgate*, 1969; *McQuillin et al.*, 1982; *Rogers et al.*, 1989;
271 *Underhill & Brodie*, 1993).

272

273 **3.3 Helmsdale**

274 Between Golspie and Helmsdale, Permo-Trias to Upper Jurassic strata crop out along
275 the Helmsdale Fault (**Figure 10**). At Helmsdale, Jurassic strata are in contact with the
276 Helmsdale Granite (Silurian-Devonian; **Figures 10 and 11**). In this area, the Jurassic strata
277 are Kimmeridgian, as at Eathie; however at Helmsdale units of conglomerate (Helmsdale
278 Boulder Beds) alternate with shale, as a result of syn-tectonic sedimentation in the footwall of
279 a normal fault (*Thiérault & Steel*, 1995; *Trewin & Hurst*, 2009). The conglomerate contains
280 Devonian clasts, indicating that Devonian strata lay above the Helmsdale Granite at the time
281 of faulting. Moreover, steep calcite veins cut the conglomerate, indicating extension in a
282 direction perpendicular to the Helmsdale Fault (**Figure 11B**). We did not find any ‘beef’ in
283 Jurassic strata at Helmsdale and this is consistent with shallow burial, by comparison with the
284 Jurassic strata at Eathie and Shandwick.

285 Another set of steep calcite veins cuts the entire sequence and therefore post-dates the
286 Jurassic. These veins are sigmoidal, indicating left-lateral slip along the Helmsdale fault zone
287 (**Figure 11**). Such a motion is compatible with right-lateral displacement on the GGF. Indeed,
288 according to previous studies, folds between the Helmsdale Fault and the GGF may have
289 developed as a result of opposing senses of slip on these two faults (*Thomson & Underhill*,
290 1993).

291

292 **4. Discussion**

293 At Eathie and Shandwick, folds, faults and veins provide structural evidence for post-
294 Jurassic right-lateral reactivation of the GGF. Furthermore, ‘beef’ at outcrop is one indication
295 that the Mesozoic strata were subject to several km of burial and then to post-Jurassic
296 exhumation. In contrast, at Helmsdale there is no ‘beef’ and Jurassic conglomerate
297 accumulated at shallower depth, in the footwall of the active Helmsdale Fault. Sigmoidal
298 calcite veins, which cut the Jurassic sequence at Helmsdale, indicate left-lateral displacement
299 on the Helmsdale Fault. This is compatible with right-lateral displacement along the GGF
300 (*Underhill & Brodie, 1993; Thomson & Underhill, 1993*). At Cadh’an-Rìgh our observations
301 provide further evidence for right-lateral reactivation of the GGF. However, the reverse
302 faulting would indicate a local context of transpression, rather than transtension.

303 Our observations show clearly that right-lateral reactivation of the GGF was post-
304 Jurassic, but we know of no younger strata onshore, other than Quaternary. Subsurface data
305 from the offshore IMF Basin and the apparent offsets of Palaeocene-Eocene dykes in NW
306 Scotland all indicate that reactivation occurred in Tertiary time (*Holgate, 1969; Underhill &*
307 *Brodie, 1993; Thomson & Underhill, 1993; Thomson & Hillis, 1995*). However, the exact
308 timing remains uncertain. *Underhill & Brodie (1993)* showed that the IMF Basin underwent
309 regional uplift during the Cenozoic and they attributed this to reactivation of the GGF. More
310 generally, periods of uplift occurred at 65-60 Ma, 40-25 Ma and 15-10 Ma and may have
311 continued into Late Neogene time (*Hall & Bishop, 2002; Holford et al., 2009, 2010*).
312 Therefore, it seems likely that reactivation of the GGF occurred during one of these periods
313 **(Figure 12)**.

314 *Hillis et al. (1994)* suggested that exhumation in the IMF occurred in mid-late Danian
315 time (65.5 – 61.7 Ma, early Palaeogene), when a major unconformity developed. As we have
316 explained earlier, a period of uplift did affect Scotland in Early Palaeogene time, probably in
317 connection with the Iceland Mantle Plume and widespread magmatic activity west of

318 Scotland. However, the GGF has offset right-laterally the Palaeocene-Eocene dykes of NW
319 Scotland. The youngest of those dykes formed at about 52 Ma (*Holgate, 1969*). Thus dextral
320 reactivation of the GGF continued after that time. Moreover, several unconformities
321 developed during the Cenozoic, in the North Sea rift system, and during the Palaeogene,
322 offshore Scotland (e.g *Evans et al., 2003; Stoker et al., 2012*). Furthermore, *Evans et al.*
323 (2003) have described several phases of local inversion in the IMF in middle Eocene,
324 Oligocene and Miocene times. Thus the significant uplift of Scotland in Early Palaeocene
325 time may have been due to processes other than tectonic reactivation. In Northern Ireland, a
326 recent high-resolution aeromagnetic survey has demonstrated that Caledonian faults
327 reactivated during Palaeogene time, and, more precisely, in Early Palaeocene and Oligocene
328 time. The latter phase was associated with the development of Oligocene pull-apart basins
329 (*Cooper et al., 2012*) and was maybe coeval with reactivation of the GGF. Thus, it is most
330 likely that reactivation of the GGF occurred in Palaeogene time (after 52 Ma).

331 Amongst the possible causes for reactivation of the GGF and for Cenozoic uplift of
332 Scotland are: (1) mantle processes from the Iceland Plume, (2) intra-plate compression from
333 the Alpine Orogeny, (3) ridge push from the NE Atlantic and (4) variations in the amount and
334 rate of sea-floor spreading in the NE Atlantic. According to recent restorations (*Le Breton et*
335 *al., 2012*), variations in the amount and direction of sea-floor spreading, between the
336 Reykjanes and Aegir ridges of the NE Atlantic (**Figure 13**), generated left-lateral
337 transpressional displacement along the FFZ, first in the Early Eocene (c. 56-51 Ma) and then
338 from the Early Eocene to Late Oligocene (c. 47-26 Ma). During the latter phase, the Jan
339 Mayen Microcontinent (JMMC) rifted progressively (from south to north) off East Greenland.
340 When these continental areas finally separated, sea-floor spreading transferred from the Aegir
341 Ridge to the Kolbeinsey Ridge (**Figures 12 and 13**). According to the stationary hot spot
342 model of *Lawver & Müller (1994)*, the head of the Iceland Plume was beneath the eastern

343 Greenland Margin at that time (*c.* 40-30 Ma). *Müller et al.* (2001) suggested that the Iceland
344 Mantle Plume was responsible for (1) rifting at the edge of the eastern Greenland margin, (2)
345 formation of the Kolbeinsey Ridge, west of Jan Mayen, (3) subsequent extinction of the Aegir
346 Ridge and (4) separation of the JMMC from Greenland.

347 The Middle Eocene to Late Oligocene was a period of uplift in Scotland and of
348 compressional deformation on the NW United Kingdom Continental Margin (**Figure 12**).
349 Numerous compressional structures developed offshore Scotland (e.g. the Wyville-Thomson,
350 Ymir ridges (WYTR), the Alpin Dome and the Judd Anticline) from the Middle Eocene to the
351 Early Miocene (**Figure 13**; *Smallwood, 2004; Johnson et al., 2005; Ritchie et al., 2008; Tuitt*
352 *et al., 2010; Stoker et al., 2012*). *Le Breton et al.* (2012) have suggested that differential sea-
353 floor spreading of NE Atlantic ridges was responsible for compressional deformation on the
354 continental margin at those times. Here we suggest furthermore that this differential sea-floor
355 spreading was also responsible for reactivation of the GGF. Indeed, a left-lateral displacement
356 along the FFZ is compatible with a right-lateral reactivation of the GGF (**Figure 13**). The
357 stress field from the Alpine Orogeny and pulses from the Iceland Mantle plume may have
358 amplified the intraplate stress in Scotland, so contributing to reactivation of the GGF. Because
359 all these processes were active simultaneously, from the Late Eocene to the Late Oligocene
360 (*c.* 37-26 Ma), we consider that reactivation of the GGF probably occurred in this interval
361 (**Figure 12**).

362

363 **Conclusions**

364 (1) Our field observations of Jurassic outcrops in Eathie, Shandwick and Helmsdale, NE
365 Scotland, provide additional evidence for post-Jurassic right-lateral reactivation of the GGF,
366 under transpression.

367 (2) The ‘beef’ structures in Jurassic shale at Eathie and Shandwick provide evidence that
368 this formation accumulated deeper offshore in the IMF Basin and has been subject to post-
369 Jurassic exhumation. This exhumation would be compatible with right-lateral displacement
370 on the GGF. Assuming that ‘beef’ structures form at approx. 1500-2500 m depth (*Rodrigues*
371 *et al.*, 2009) and from the 8° pitch of striae on fault planes at Cadh’-an-Righ, we estimate that
372 right-lateral displacement along the GGF was in the order of 10-18 km.

373 (3) The timing of reactivation of the GGF remains uncertain; however we suggest that the
374 GGF reactivated right-laterally in a time interval from Late Eocene to Late Oligocene, *c.* 37 to
375 26 Ma. This period coincides with (1) an uplift episode of Scotland, (2) intraplate stress from
376 the Alpine Orogeny (3) a pulse of the Iceland Mantle Plume, and more importantly with (4)
377 left-lateral slip along the FFZ due to differential sea-floor spreading and plate readjustment in
378 the NE Atlantic (separation of the JMMC, ‘ridge jump’ from the Aegir to the Kolbeinsey
379 ridges). Indeed, left-lateral slip along the FFZ is compatible with right-lateral reactivation of
380 the GGF.

381 (4) In the future, low-temperature geochronological studies may provide better constraints
382 on the timing of reactivation of the GGF. However, the vertical motion along the GGF may
383 not have been significant enough to be detectable in such studies. Similar work along the
384 MTF, Norway, would provide better constraints on the relationships between differential
385 spreading along the NE Atlantic, left-lateral slip along the FFZ and JMFZ, uplift of Scotland
386 and Norway, and Tertiary reactivation of the GGF and MTF.

387

388 **Acknowledgements**

389 We would like to thank Chevron USA for funding the PhD project of E. Le Breton and in
390 particular Gavin Lewis and Peter Connolly for instigating the project. We are grateful to

391 Andrew Hurst and John Parnell for providing maps, publications, data and encouragement,
392 during our visit to Aberdeen University in August 2011. We also thank Marc Jolivet of the
393 University of Rennes 1 for information on reactivation of the GGF. Finally, we thank Andrew
394 Hurst and Howard Johnson for their helpful reviews.

395

396

397 **References**

- 398 Argent, J.D., Stewart, S.A., Green, P.F. & Underhill, J.R., 2002. Heterogeneous exhumation
399 in the Inner Moray Firth, UK North Sea: constraints from new AFTA(R) and seismic
400 data. *Journal of the Geological Society*, **159**(6), 715-729, doi:10.1144/0016-764901-141.
- 401 Boldreel, L.O., & Andersen, M.S., 1993. Late Pliocene to Miocene compression in the
402 Faeroe-Rockall area. In: Parker, J.R. (eds), *Petroleum Geology of Northwest Europe:
403 Proceedings of the 4th Conference*, Geological Society, London, Petroleum Geology
404 Conference series, **4**, 1025-1034.
- 405 Boldreel, L.O. & Andersen, M.S., 1998. Tertiary compressional structures on the Faroe –
406 Rockall Plateau in relation to northeast Atlantic ridge-push and Alpine foreland stresses.
407 *Tectonophysics*, **300**, 13-28.
- 408 Brekke, H., 2000. The tectonic evolution of the Norwegian Sea Continental Margin with
409 emphasis on the Vøring and More Basins. In: Nøttvedt, A. (eds), *Dynamics of the
410 Norwegian Margin*, Geological Society, London, Special Publications, **167**, 327-378.
- 411 Brodie, J. & White N., 1994. Sedimentary basin inversion caused by igneous underplating:
412 Northwest European continental shelf. *Geology*, **22**, 147-150.
- 413 Clift, P.D., Carter, A. & Hurford, A.J., 1998. The erosional and uplift history of NE Atlantic
414 passive margins: constraints on a passing plume. *Journal of the Geological Society,
415 London*, **155**, 787-800.
- 416 Cooper, M.R., Anderson, H., Walsh, J.J., Cab Dan, C.L., Young, M.E., Earl, G. & Walker,
417 A. (2012). Palaeogene Alpine tectonics and Icelandic plume-related magmatism and
418 deformation in Northern Ireland. *Journal of the Geological Society, London*, **169**, 29-36,
419 doi: 10.1144/0016-76492010-182.
- 420 Doré, A.G., Lundin, E.R., Kuszniir, N.J. & Pascal C., 2008. Potential mechanisms for the
421 genesis of Cenozoic domal structures on the NE Atlantic margin: pros, cons and some
422 new ideas. In: Johnson, H., Doré, A.G., Gatliff, R.W., Holdsworth, R., Lundin, E.R. &
423 Ritchie, J.D. (eds), *The Nature and Origin of Compression in Passive Margins*,
424 Geological Society, London, Special Publications, **306**, 1-26.
- 425 Evans, D., Graham, C., Armour, A. & Bathurst P., 2003. *The Millennium Atlas: petroleum
426 geology of the central and northern North Sea*. Geological Society, London, 389 p.
- 427 Firth, C.R. & Stewart, I.S., 2000. Postglacial tectonics of the Scottish glacio-isostatic uplift
428 centre. *Quaternary Science Reviews*, **19**, 1469-1493.
- 429 Hall, A. & Bishop P., 2002. Scotland's denudational history: an integrated view of erosion
430 and sedimentation at an uplifted passive margin. In: Doré, A.G., Cartwright, J.A., Stoker,
431 M.S., Turner, J.P. & White, N. (eds), *Exhumation of the North Atlantic Margin: Timing*,

- 432 *Mechanisms and Implications for Petroleum Exploration*, Geological Society, London,
433 Special Publications, **196**, 271-290.
- 434 Hillier, R.D. & Cosgrove, J.W., 2002. Core and seismic observations of overpressure-related
435 deformation within Eocene sediments of the Outer Moray Firth, UKCS. *Petroleum*
436 *Geoscience*, **8**, 141-149.
- 437 Hillis, R.R., Thomson, K. & Underhill, J.R., 1994. Quantification of Tertiary erosion in the
438 Inner Moray Firth using sonic velocity data from the Chalk and the Kimmeridge Clay.
439 *Marine and Petroleum Geology*, **11(3)**, 283-293.
- 440 Hitchen, K. 2004. The geology of the UK Hatton-Rockall margin. *Marine and Petroleum*
441 *Geology*, **21**, 993-1012, doi:10.1016/j.marpetgeo.2004.05.004.
- 442 Holford, S.P., Green, P.F., Duddy, I.R., Turner, J.P., Hillis, R.R. & Stoker, M.S., 2009.
443 Regional intraplate exhumation episodes related to plate-boundary deformation.
444 *Geological Society of America Bulletin*, **121(11-12)**, 1611-1628, doi:10.1130/B26481.1.
- 445 Holford, S. P., Green, P.F., Hillis, R.R., Underhill, J.R., Stoker, M.S. & Duddy, I.R., 2010.
446 Multiple post-Caledonian exhumation episodes across NW Scotland revealed by apatite
447 fission-track analysis. *Journal of the Geological Society*, **167(4)**, 675-694,
448 doi:10.1144/0016-76492009-167.
- 449 Holgate, N., 1969. Palaeozoic and Tertiary transcurrent movements on the Great Glen Fault.
450 *Scottish Journal of Geology*, **5(2)**, 97-139.
- 451 Hutton, D.H.W. & McErlean, M., 1991. Silurian and Early Devonian sinistral deformation of
452 the Ratagain granite, Scotland: constraints on the age of Caledonian movements on the
453 Great Glen fault system. *Journal of the Geological Society, London*, **148**, 1-4.
- 454 Institute of Geological Sciences, 1973. *Geological Map of Cromarty, Sheet 94, 1:50 000*.
455 British Geological Survey.
- 456 Johnson, H., Ritchie, J. D., Hitchen, K., McInroy, D. B. & Kimbell, G.S., 2005. Aspects of the
457 Cenozoic deformational history of the Northeast Faroe – Shetland Basin, Wyville –
458 Thomson Ridge and Hatton Bank areas. In: Doré, A.G. & Vining, B.A. (eds), *Petroleum*
459 *Geology: North-West Europe and Global Perspectives - Proceedings of the 6th*
460 *Petroleum Geology Conference*, Geological Society, London, Petroleum Geology
461 Conference series, **6**, 993-1007.
- 462 Jolivet, M., 2007. Histoire de la dénudation dans le corridor du loch Ness (Écosse) :
463 mouvements verticaux différentiels le long de la Great Glen Fault. *Comptes Rendus*
464 *Geosciences*, **339(2)**, 121-131, doi:10.1016/j.crte.2006.12.005.
- 465 Jones, S.M., White, N., Clarke, B.J., Rowley, E. & Gallagher, K., 2002. Present and past
466 influence of the Iceland Plume on sedimentation. In: Doré, A.G., Cartwright, J.A., Stoker,
467 M.S., Turner, J.P. & White, N. (eds), *Exhumation of the North Atlantic Margin: Timing*,

- 468 *Mechanisms and Implications for Petroleum Exploration*, Geological Society, London,
469 Special Publications, **196**, 13-25.
- 470 Jonk, R., Duranti, D., Parnell, J., Hurst, A. & Fallick, A.E., 2003. The structural and
471 diagenetic evolution of injected sandstones: examples from the Kimmeridgian of NE
472 Scotland. *Journal of the Geological Society, London*, **160**, 881-894.
- 473 Judd, J.W., 1873. The Secondary Rocks of Scotland. *Quarterly Journal of the Geological*
474 *Society*, **29**(1-2), 97-195, doi:10.1144/GSL.JGS.1873.029.01-02.16.
- 475 Lawver, L.A., & Müller, R.D., 1994. Iceland Hotspot track, *Geology*, **22**, 311-314.
- 476 Le Breton, E., Cobbold, P.R., Dauteuil, O. & Lewis, G., 2012. Variations in amount and
477 direction of sea-floor spreading along the North East Atlantic Ocean and resulting
478 deformation of the continental margin of North West Europe. *Tectonics*, **31**, TC5006,
479 doi:10.1029/2011TC003087.
- 480 Lundin, E.R. & Doré, A.G., 2002. Mid-Cenozoic post-breakup deformation in the “passive”
481 margins bordering the Norwegian - Greenland Sea. *Marine and Petroleum Geology*, **19**,
482 79-93.
- 483 Mackay, L.M., Turner, J., Jones, S.M. & White N.J., 2005. Cenozoic vertical motions in the
484 Moray Firth Basin associated with initiation of the Iceland Plume. *Tectonics*, **24**(5), 1-23,
485 doi:10.1029/2004TC001683.
- 486 McQuillin, R., Donato, J.A. & Tulstrup J., 1982. Development of basins in the Inner Moray
487 Firth and the North Sea by crustal extension and dextral displacement of the Great Glen
488 Fault, *Earth and Planetary Science Letters*, **60**, 127-139.
- 489 Mendum, J.R. & Noble, S.R., 2010. Mid-Devonian sinistral transpressional movements on the
490 Great Glen Fault: the rise of the Rosemarkie Inlier and the Acadian event in Scotland. In:
491 Law, R.D, Butler, R.W.H., Holdsworth, R.E., Krabbendam, M., Strachan, R.A. (eds),
492 *Continental tectonics and mountain building: the legacy of Peach and Horne*, Geological
493 Society, London, Special Publications, **335**, 161-187.
- 494 Miller, H., 1851. *The old red sandstone or, New walks in an old field*, published by Gould and
495 Lincoln, Boston, 288 p. From the 4th London Edition.
- 496 Mosar, J., Lewis, G. & Torsvik, T., 2002. North Atlantic sea-floor spreading rates:
497 implications for the Tertiary development of inversion structures of the Norwegian –
498 Greenland Sea. *Journal of the Geological Society*, **159**, 503-515, doi:110.1144/0016-
499 764901-135.
- 500 Müller, R.D., Gaina, C., Roest, W.R. & Hansen, D.L., 2001. A recipe for microcontinent
501 formation, *Geology*, **29**(3), 203.
- 502 Nadin, P.A., Kusznir, N.J. & Cheadle, M.J., 1997. Early Tertiary plume uplift of the North
503 Sea and Faeroe-Shetland Basins. *Earth and Planetary Science Letters*, **148**, 109-127.

- 504 Persano, C., Barfod, D.N., Stuart, F.M. & Bishop, P., 2007. Constraints on early Cenozoic
505 underplating-driven uplift and denudation of western Scotland from low temperature
506 thermochronometry. *Earth and Planetary Science Letters*, **263**(3-4), 404-419,
507 doi:10.1016/j.epsl.2007.09.016.
- 508 Richard, P., Mocquet, B. & Cobbold, P.R., 1991. Experiments on simultaneous faulting and
509 folding above a basement wrench fault. *Tectonophysics*, **188**, 133-141.
- 510 Ritchie, J.D., Johnson, H. & Kimbell G.S., 2003. The nature and age of Cenozoic
511 contractional deformation within the NE Faroe–Shetland Basin. *Marine and Petroleum*
512 *Geology*, **20**(5), 399-409, doi:10.1016/S0264-8172(03)00075-8.
- 513 Ritchie, J.D., Johnson, H., Quinn, M.F. and Gatliff, R.W., 2008. The effects of Cenozoic
514 compression within the Faroe-Shetland Basin and adjacent areas. In: Johnson, H., Doré,
515 A.G., Gatliff, R.W., Holdsworth, R., Lundin, E.R. & Ritchie, J.D. (eds), *The Nature and*
516 *Origin of Compression in Passive Margins*, **306**, 121-136, Geological Society, London,
517 Special Publications.
- 518 Roberts, D.G., 1989. Basin inversion in and around the British Isles. *Geological Society,*
519 *London, Special Publications*, **44**(1), 131-150, doi:10.1144/GSL.SP.1989.044.01.09.
- 520 Rodrigues, N., Cobbold, P.R., Loseth, H. & Ruffet, G., 2009. Widespread bedding-parallel
521 veins of fibrous calcite ('beef') in a mature source rock (Vaca Muerta Fm, Neuquen
522 Basin, Argentina): evidence for overpressure and horizontal compression. *Journal of the*
523 *Geological Society, London*, **166**(4), 695-709.
- 524 Rogers, D.A., Marshall, J.E.A. and Austin T.R., 1989. Devonian and later movements on the
525 Great Glen fault system, Scotland. *Journal of the Geological Society, London*, **146**, 369-
526 372.
- 527 Saunders, A.D., Fitton, J.G., Kerr, A.C., Norry, M.J. & Kent, R.W., 1997. The North Atlantic
528 Igneous Province. In: Mahoney, J.J. & Coffin, M.F. *Large Igneous Provinces*
529 *Continental, Oceanic, and Planetary Flood Volcanism*, Geophysical Monograph, **100**,
530 45-93.
- 531 Saunders, A.D., Jones, S.M., Morgan, L.A., Pierce, K.L., Widdowson, M. & Xu, Y.G., 2007.
532 Regional uplift associated with continental large igneous provinces: The roles of mantle
533 plumes and the lithosphere. *Chemical Geology*, **241**(3-4), 282-318,
534 doi:10.1016/j.chemgeo.2007.01.017.
- 535 Selley, R.C., 1992. Petroleum seepages and impregnations in Great Britain. *Marine and*
536 *Petroleum Geology*, **9**, 226-244.
- 537 Smallwood, J.R., 2004. Tertiary Inversion in the Faroe-Shetland Channel and the
538 Development of Major Erosional Scarps. *Geological Society, London, Memoirs*, **29**(1),
539 187-198, doi:10.1144/GSL.MEM.2004.029.01.18.

- 540 Soper, N.J., Strachan, R.A., Holdsworth, R.E., Gayer, R.A. & Geiling R.O., 1992. Sinistral
541 transpression and the Silurian closure of Iapetus. *Journal of the Geological Society*,
542 *London*, **149**, 871-880.
- 543 Speight, J.M. & Mitchell, J.G., 1979. The Permo-Carboniferous dyke-swarm of northern
544 Argyll and its bearing on dextral displacement on the Great Glen Fault. *Journal of the*
545 *Geological Society, London*, **139**, 3-11.
- 546 Stewart, M., Holdsworth, R.E. & Strachan, R.A., 2000. Deformation processes and
547 weakening mechanisms within the frictional \pm viscous transition zone of major crustal-
548 scale faults: insights from the Great Glen Fault Zone, Scotland. *Journal of Structural*
549 *Geology*, **22**, 543-560.
- 550 Stewart, M., Strachan, R.A., Martin, M.W. & Holdsworth, R.E., 2001. Constraints on early
551 sinistral displacements along the Great Glen Fault Zone, Scotland: structural setting, U-
552 Pb geochronology and emplacement of the syn-tectonic Clunes tonalite. *Journal of the*
553 *Geological Society*, **158**(5), 821-830, doi:10.1144/jgs.158.5.821.
- 554 Stoker, M.S., 2002. Late Neogene development of the UK Atlantic Margin. In: Doré, A.G.,
555 Cartwright, J.A., Stoker, M.S., Turner, J.P. & White, N. (eds), *Exhumation of the North*
556 *Atlantic Margin: Timing, Mechanisms and Implications for Petroleum Exploration*,
557 Geological Society, London, Special Publications, **196**, 313-329.
- 558 Stoker, M.S., Hoult, R.J., Nielsen, T., Hjelstuen, B.O., Laberg, J.S. & Shannon P.M., 2005.
559 Sedimentary and oceanographic responses to early Neogene compression on the NW
560 European margin. *Atlantic*, **22**, 1031-1044, doi:10.1016/j.marpetgeo.2005.01.009.
- 561 Stoker M.S., Kimbell G.S., McNroy D.B. & Morton A.C., 2012. Eocene post-rift
562 tectonostratigraphy of the Rockall Plateau, Atlantic margin of NW Britain: Linking early
563 spreading tectonics and passive margin response. *Marine and Petroleum Geology*, **30**, 98-
564 125.
- 565
566 Stone, P., 2007. *Bedrock geology UK North, An explanation of the bedrock geology map of*
567 *Scotland, northern England, Isle of Man and Northern Ireland - 1:625 000*, 5th Edition,
568 British Geological Survey, Natural Environment Research Council.
- 569 Sykes, R.M., 1975. The stratigraphy of the Callovian and Oxfordian stages (Middle-Upper
570 Jurassic) in northern Scotland. *Scottish Journal of Geology*, **11**(1), 51-78.
- 571 Thiéroult, P. & Steel, R.J., 1995. Syn-rift sedimentation in the Upper Jurassic (Helmsdale
572 Boulder Beds) of the Inner Moray Firth. In: Steel, R.J., Felt, V.L., Johannessen, E.P. &
573 Mathieu, C. (eds), *Sequence Stratigraphy on the Northwest European Margin*, **5**, 365-
574 387, Norwegian Petroleum Society Special Publication.
- 575 Thomson, K. & Hillis, R.R., 1995. Tertiary structuration and erosion of the Inner Moray Firth.
576 In: Scrutton, R.A., Stoker, M.S., Shimmield, G.B. & Tudhope, A.W. (eds), *The*

- 577 *Tectonics, Sedimentation and Palaeoceanography of the North Atlantic Region,*
578 Geological Society, London, Special Publications, **90**, 249-269.
- 579 Thomson, K., & Underhill J.R., 1993. Controls on the development and evolution of
580 structural styles in the Inner Moray Firth Basin. *In: Parker, J.R. (eds), Petroleum*
581 *Geology of Northwest Europe: Proceedings of the 4th Conference*, Geological Society,
582 London, Petroleum Geology Conference series, **4**, 1167-1178.
- 583 Trewin, N.H. & Hurst, A., 2009. *Excursion Guide to the Geology of East Sutherland and*
584 *Caithness*, 2nd Edition, Aberdeen Geological Society.
- 585 Tuitt, A., Underhill, J.R., Ritchie, J.D., Johnson, H. & Hitchen, K., 2010. Timing, controls
586 and consequences of compression in the Rockall – Faroe area of the NE Atlantic Margin.
587 *In: Vining, B.A. & Pickering, S.C. (eds), Petroleum Geology: From Mature Basins to*
588 *New Frontiers - Proceedings of the 7th Petroleum Geology Conference*, Geological
589 Society, London, Petroleum Geology Conference series, **7**, 963-977.
- 590 Underhill, J.R., 1991a. Controls on Late Jurassic seismic sequences, Inner Moray Firth, UK
591 North Sea: a critical test of key segments of Exxon's original global cycle chart. *Basin*
592 *Research*, **3**, 79-98.
- 593 Underhill, J.R., 1991b. Implications of Mesozoic-Recent basin development in the western
594 Inner Moray Firth, UK. *Marine and Petroleum Geology*, **8**, 359-369.
- 595 Underhill, J.R. & Brodie, J.A., 1993. Structural geology of Easter Ross, Scotland:
596 implications for movement on the Great Glen fault zone. *Journal of the Geological*
597 *Society, London*, **150**(3), 515-527, doi:10.1144/gsjgs.150.3.0515.
- 598 White, N. & Lovell, B., 1997. Measuring the pulse of a plume with the sedimentary record.
599 *Nature*, **387**, 888-891.
- 600 White, R. & McKenzie, D., 1989. Magmatism at Rift Zones: The Generation of Volcanic
601 Continental Margins and Flood Basalts. *Journal of Geophysical Research*, **94**(B6),
602 7685-7729, doi:10.1029/JB094iB06p07685.
- 603 Wright, J.K. & Cox, B.M., 2001. British Upper Jurassic Stratigraphy (Oxfordian to
604 Kimmeridgian), *Geological Conservation Review Series*, Joint Nature Conservation
605 Committee, Peterborough, **21**, 266 p.
- 606

Figure Captions

607

608

609 **Figure 1.** Simplified geological map of northern Scotland (modified after *Stone, 2007*).

610 **Figure 2.** Top left: structural map of the North Sea Basin and location of the Inner Moray
611 Firth (IMF) Basin (modified after *Underhill, 1991a*). Top right: structural map of IMF Basin
612 (modified after *Evans et al., 2003*). Gray lines indicate locations of seismic profiles A and B.
613 A. Seismic profile of IMF Basin showing post-Cretaceous inversion structure along Wick
614 Fault at its intersection with Great Glen Fault (from *Thomson & Underhill, 1993*). B.
615 Geoseismic section showing a typical ‘flower structure’ of Great Glen Fault (from *Underhill*
616 *& Brodie, 1993*).

617 **Figure 3.** Geological map of NE Scotland (modified from *Stone, 2007*). Rectangles indicate
618 locations of figures 4-6, 7-9 and 10-11.

619 **Figure 4.** Geological map of Eathie (modified after *Institute of Geological Sciences, Sheet 94,*
620 *1973*). Strike and dip of Jurassic strata are variable, as a result of folding next to Great Glen
621 Fault (GGF). Stereonets (lower hemisphere) show poles to strata; great circles are
622 perpendicular to fold axes. Stars indicate locations of photographs in Figure 5.

623 **Figure 5.** Photographs of Jurassic outcrop at Eathie. A. Contact between Jurassic strata and
624 Devonian Old Red Sandstone in north east area. B. Contact between Jurassic strata and
625 Neoproterozoic basement in south west area. C. Fold in Jurassic strata adjacent to Great Glen
626 Fault . D. Calcite veins right-laterally offsetting Jurassic strata and striking parallel to GGF
627 (approx. N040°).

628 **Figure 6.** Photographs of ‘cone-in-cone’ (A and B) and ‘beef’ calcite cement (B) in Jurassic
629 shale at Eathie. C. Interpretation of structures in B.

630 **Figure 7.** Geological map of Shandwick (modified after *Institute of Geological Sciences,*
631 *Sheet 94, 1973*). Strike and dip of Jurassic strata are variable at Port-an-Righ and Cadh'-an-
632 Righ because of folding next to Great Glen Fault (GGF). A stereonet for Port-an-Righ (lower
633 hemisphere, right) shows poles to strata; great circle is perpendicular to nearly horizontal fold
634 axis, but some data deviate from this. Stereonet for Cadh-an-Righ (lower hemisphere, left)
635 shows great circles (for bedding planes) intersecting at steep fold axis. Stars indicate locations
636 of photographs (Figures 8 and 9).

637 **Figure 8.** Photographs of Jurassic outcrop at Port-an-Righ. A. Panoramic view that shows the
638 sigmoidal shape of Jurassic folds next to Great Glen Fault (GGF). This shape is diagnostic of
639 right-lateral slip along GGF. B. Calcite veins right-laterally offsetting Jurassic strata. C. Fault
640 contact between Jurassic and Devonian strata.

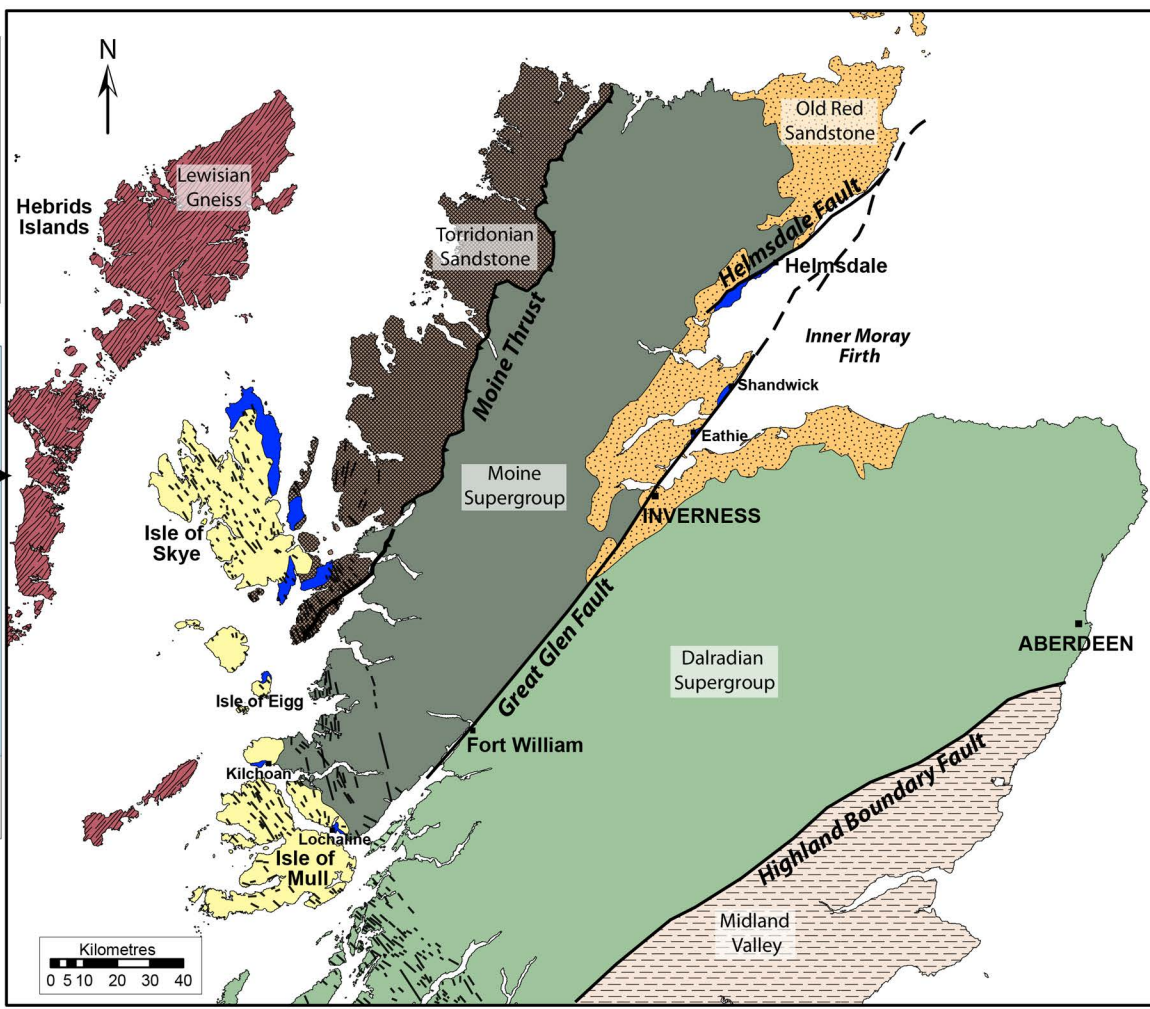
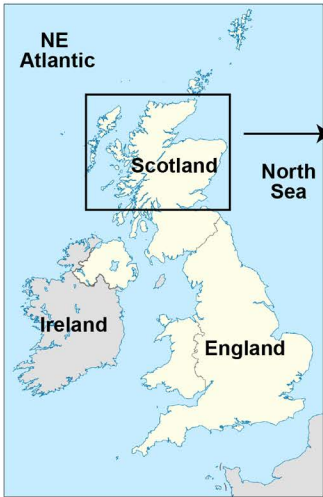
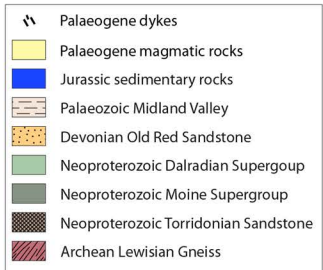
641 **Figure 9.** Photographs of Jurassic outcrop at Cadh-an-Righ. A. Wide-angle view of fault
642 contact between Jurassic and Devonian strata. B. Close-up view of same showing reverse and
643 right-lateral slip along GGF. C. 'Beef' in Jurassic shale. D. Fragment of Jurassic coal next to
644 GGF.

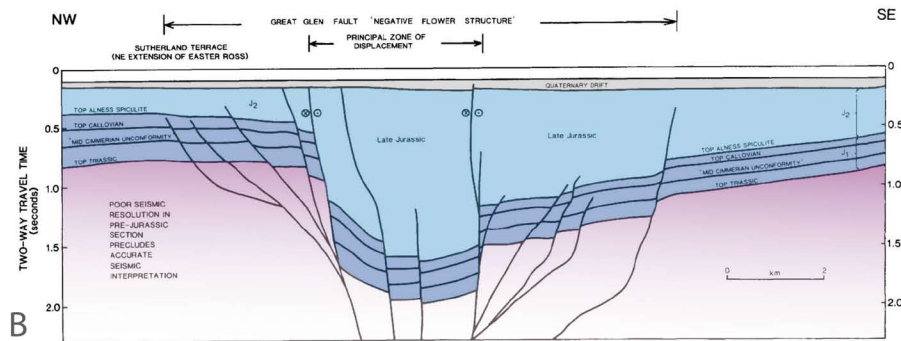
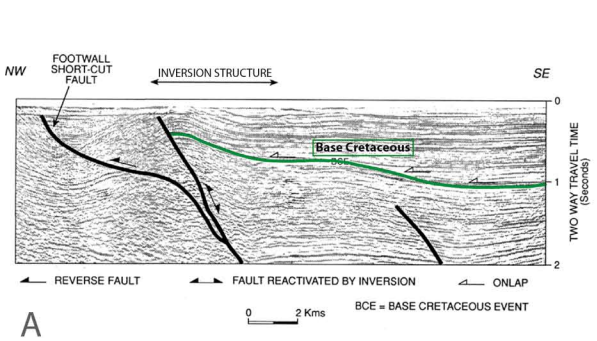
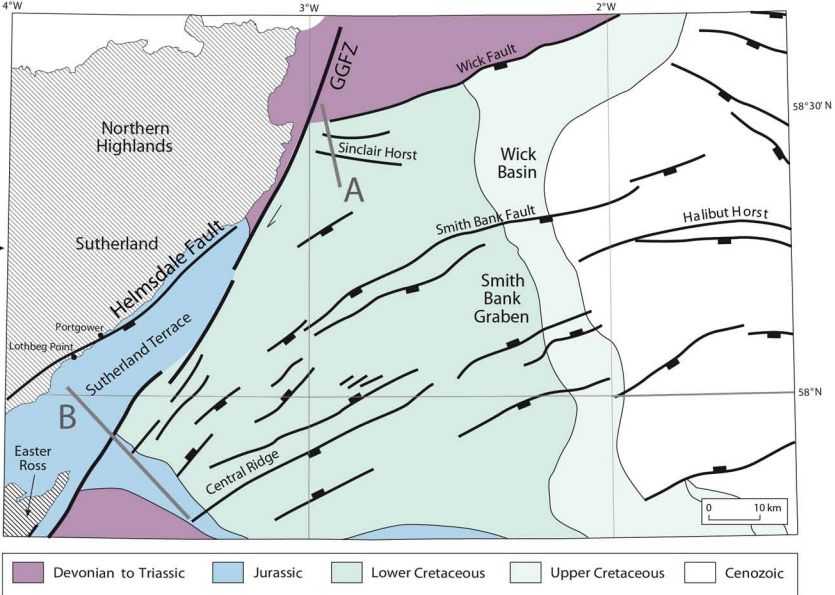
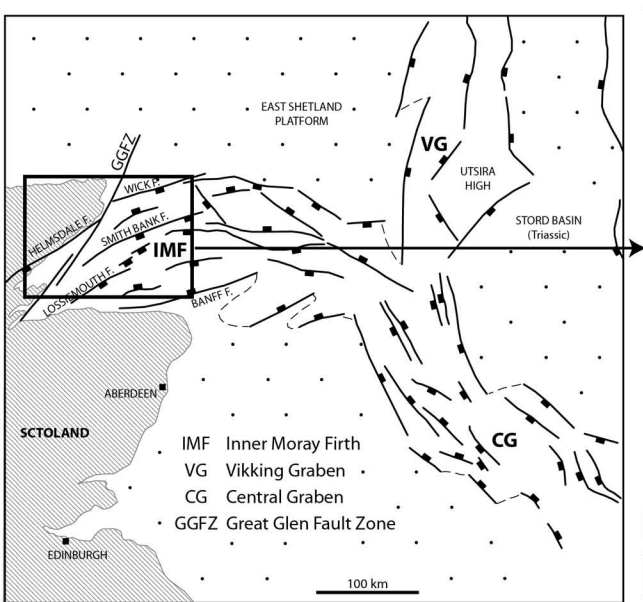
645 **Figure 10.** Geological map of Helmsdale (modified after *Stone, 2007*). Strike and dip of
646 Jurassic strata are variable as a result of folding next to Great Glen Fault (GGF). Stereonets
647 for Golspie and Helmsdale (lower hemisphere) show great circles (for bedding planes) that
648 intersect at shallowly-plunging fold axes. Stars indicate locations of photographs (Figure 11).

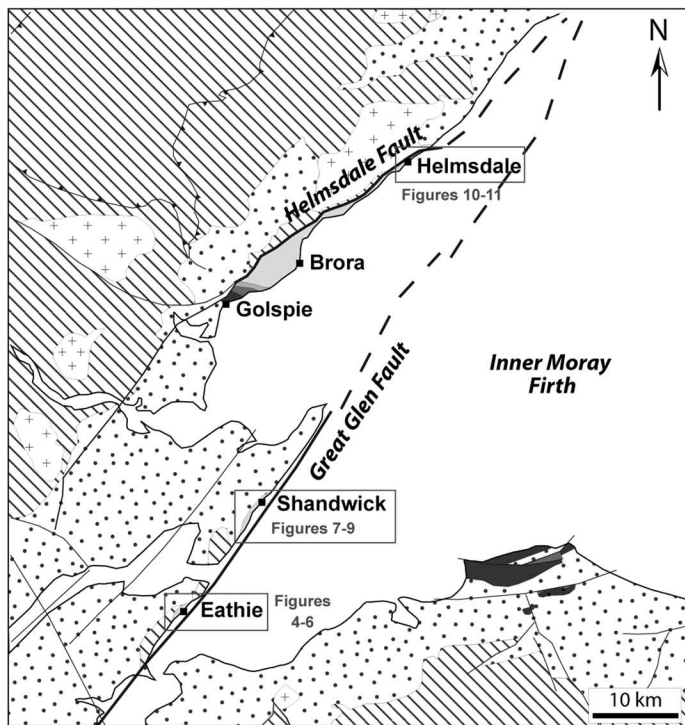
649 **Figure 11.** Photographs of Jurassic outcrop near Helmsdale. A. Jurassic 'Boulder Beds' in
650 contact with Helmsdale Granite. B. Syn-tectonic Jurassic conglomerate containing clasts of
651 Devonian strata and extensional calcite veins. C. Sigmoidal calcite veins left-laterally
652 offsetting Jurassic strata and striking parallel to Helmsdale Fault.

653 **Figure 12.** Summary and correlation of events. Numbers refer to (1) post-breakup
654 compressional deformation offshore Scotland (*Smallwood et al.*, 2004; *Johnson et al.*, 2005;
655 *Richie et al.*, 2008; *Tuitt et al.*, 2010); (2) main phases of uplift in Scotland during Cenozoic
656 time (*Hall & Bishop*, 2002; *Holford et al.*, 2009); (3) sea-floor spreading along NE Atlantic
657 ridge system, differential sea-floor spreading along NE Atlantic that resulted in left-lateral slip
658 along Faroe Fracture Zone (FFZ) and Jan Mayen Fracture Zone (JMFZ) (*Le Breton et al.*,
659 2012), ridge push, Iceland Mantle Plume pulse (correlation between age of V-shaped ridges
660 and plume pulses from *White & Lovell*, 1997), development of Iceland Plateau, and
661 compressional Alpine and Pyrenean stress field (*Tuitt et al.*, 2010). Period of synchronous
662 events (hachured) may represent timing of reactivation of Great Glen Fault (GGF). For
663 locations of post-breakup compressional structures offshore Scotland, see Figure 13.

664 **Figure 13.** Position of Europe at 36.6 Ma (Late Eocene) relative to a stationary Greenland
665 plate. According to a new method of restoration differential sea-floor spreading along
666 Reykjanes, Aegir and Mohns ridges generated left-lateral displacements along Faroe and Jan
667 Mayen fracture zones (*Le Breton et al.*, 2012). Such displacements are compatible with right-
668 lateral reactivation of Great Glen Fault and possibly of Møre Trøndelag Fault, respectively.
669 Abbreviations: AD, Alpin Dome; AR, Aegir Ridge; JA, Judd Anticline; MR, Mohns Ridge;
670 RR, Reykjanes Ridge; YR, Ymir Ridge; WTR, Wyville-Thomson Ridge. Map projection is
671 Universal Transverse Mercator (UTM, WGS 1984, zone 27N).

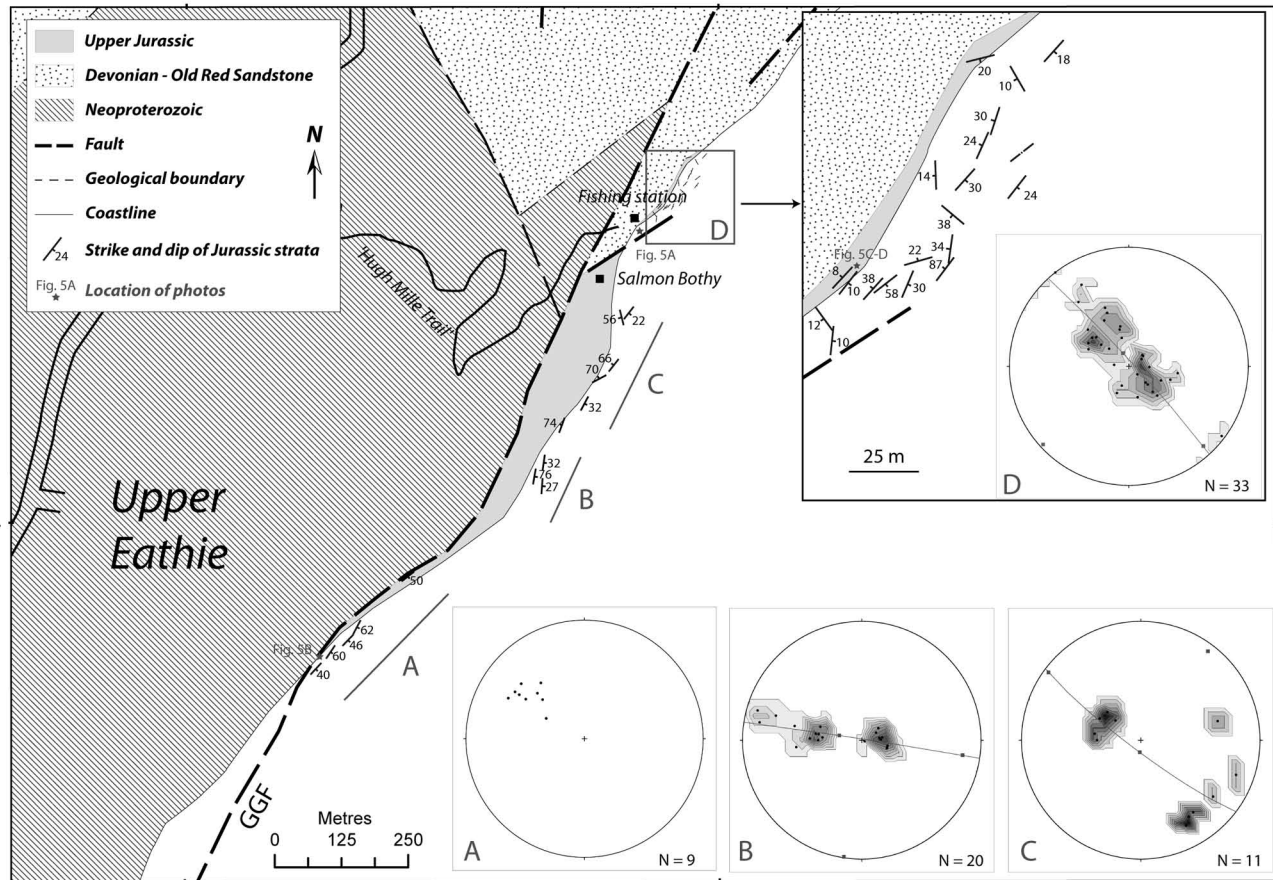






277,000 m.E.

278,000 m.E.



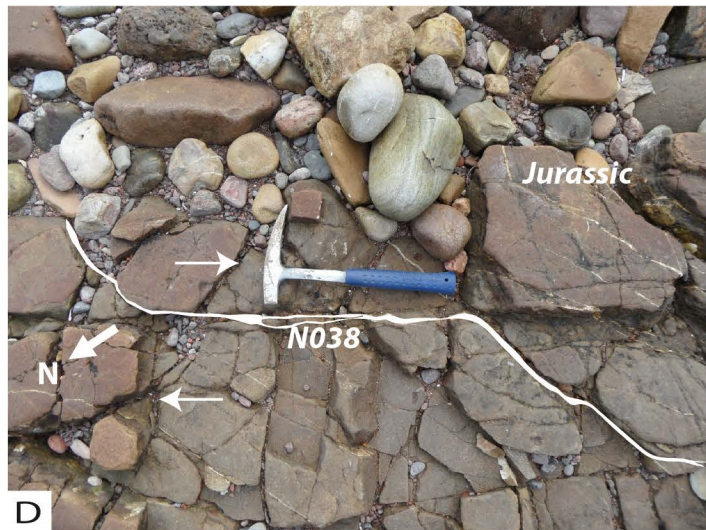
NW

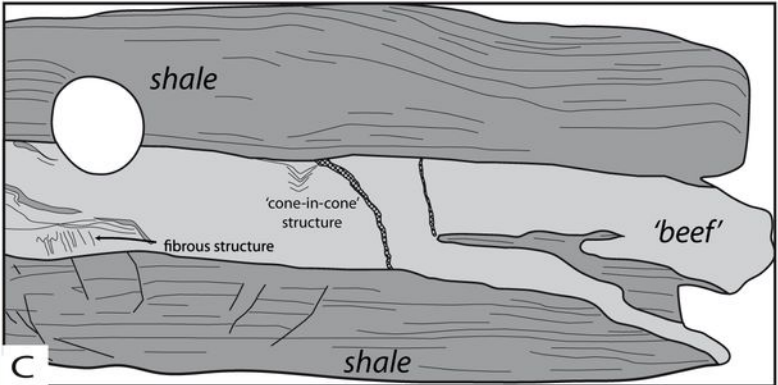
SE



SE

NW



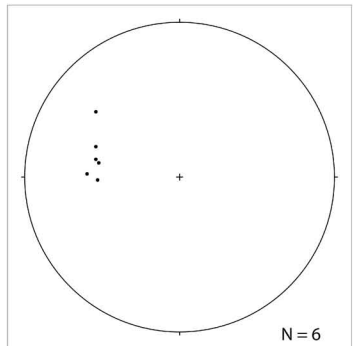
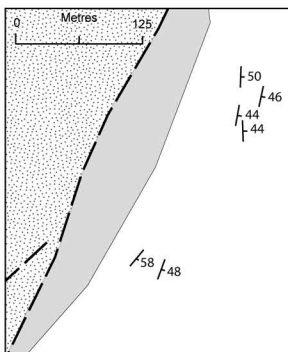
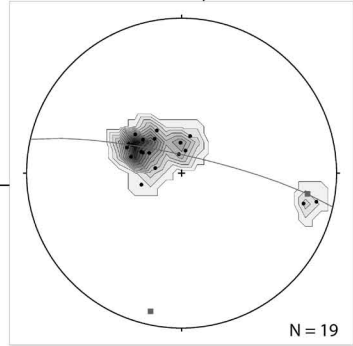
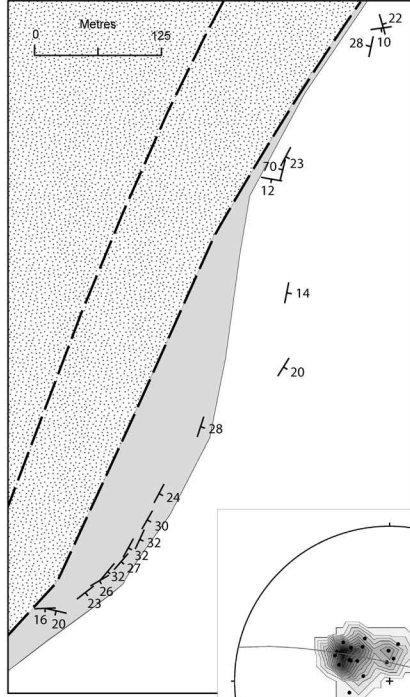
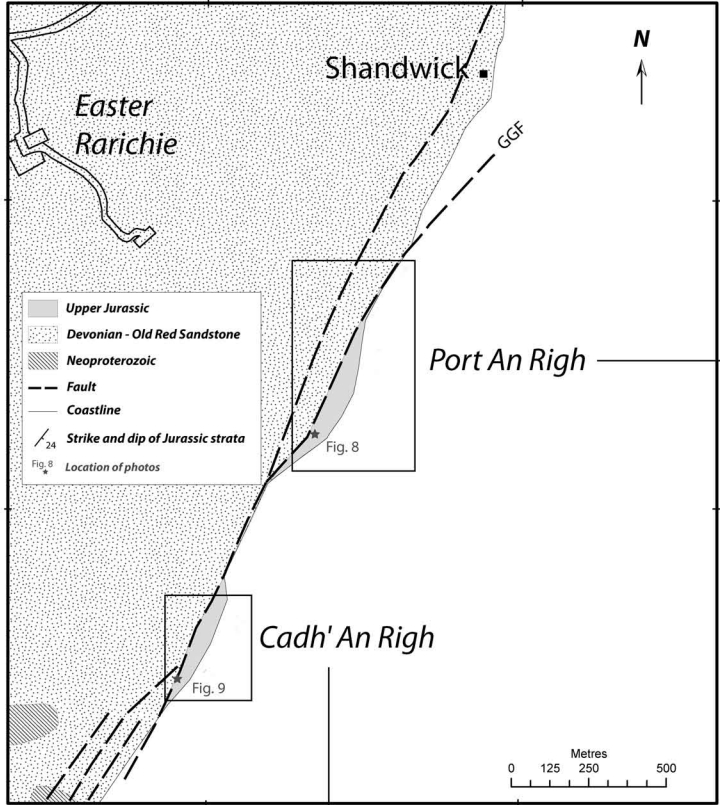


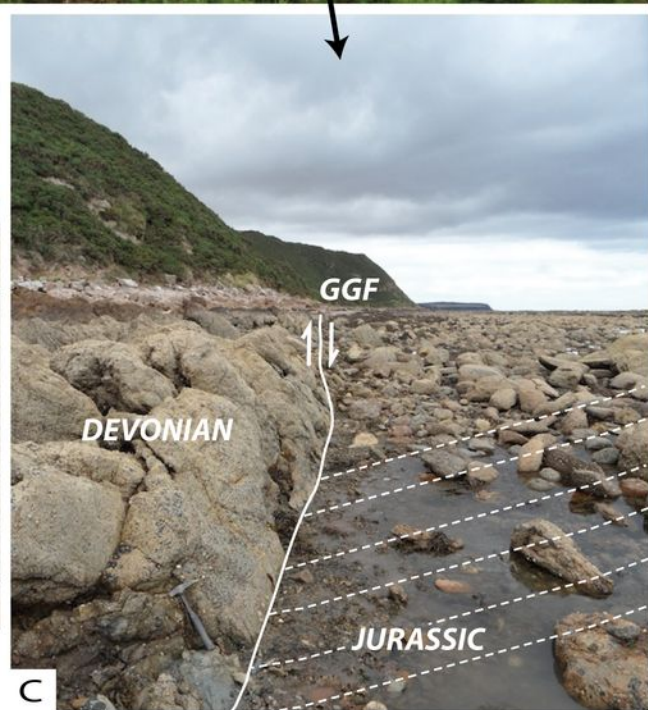
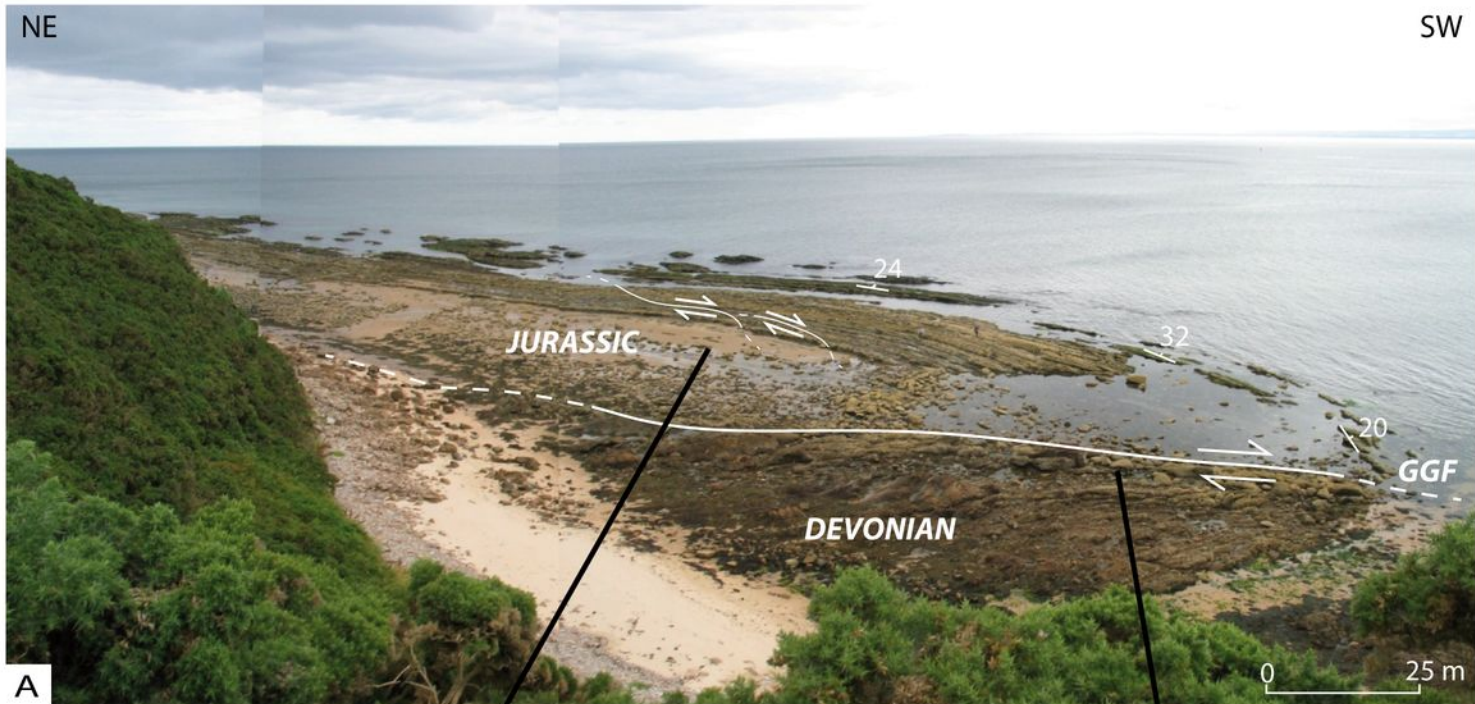
285,000 m.E.

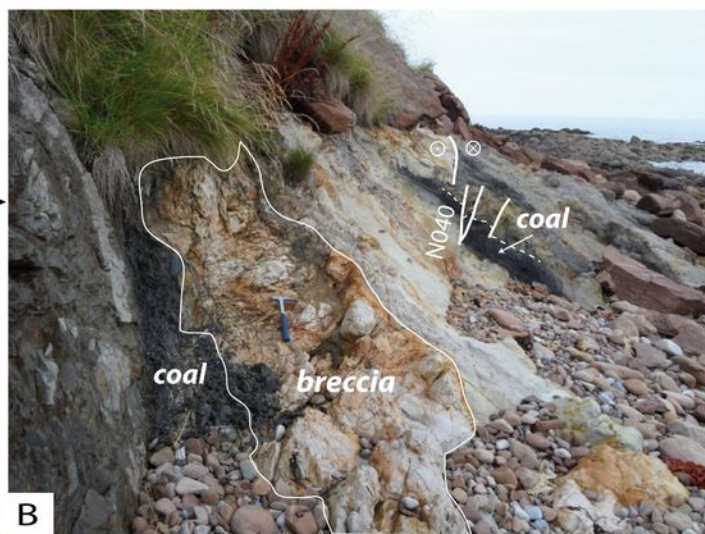
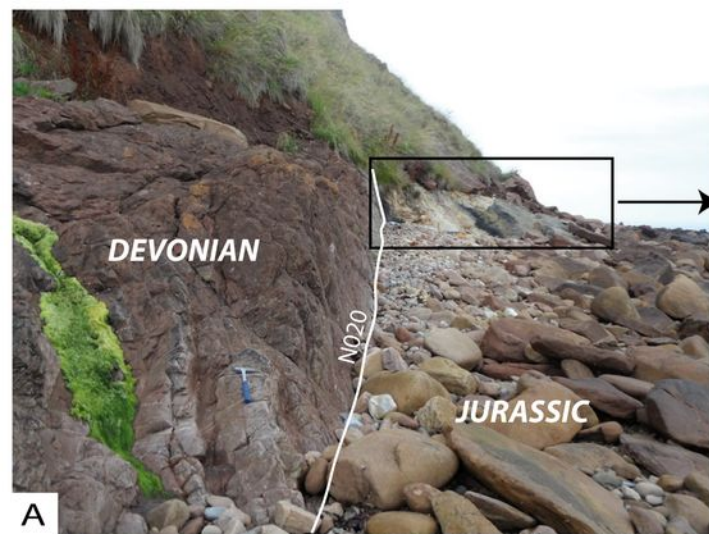
286,000 m.E.

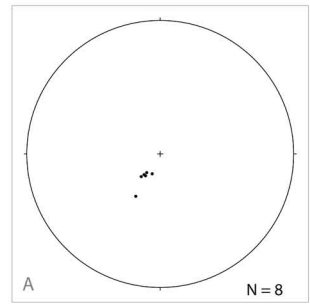
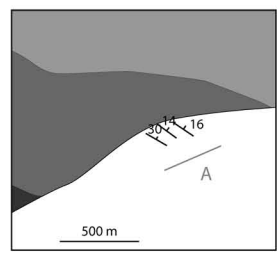
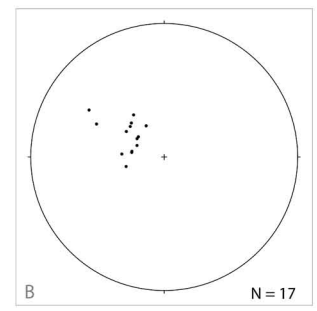
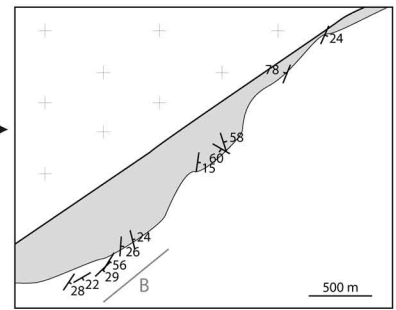
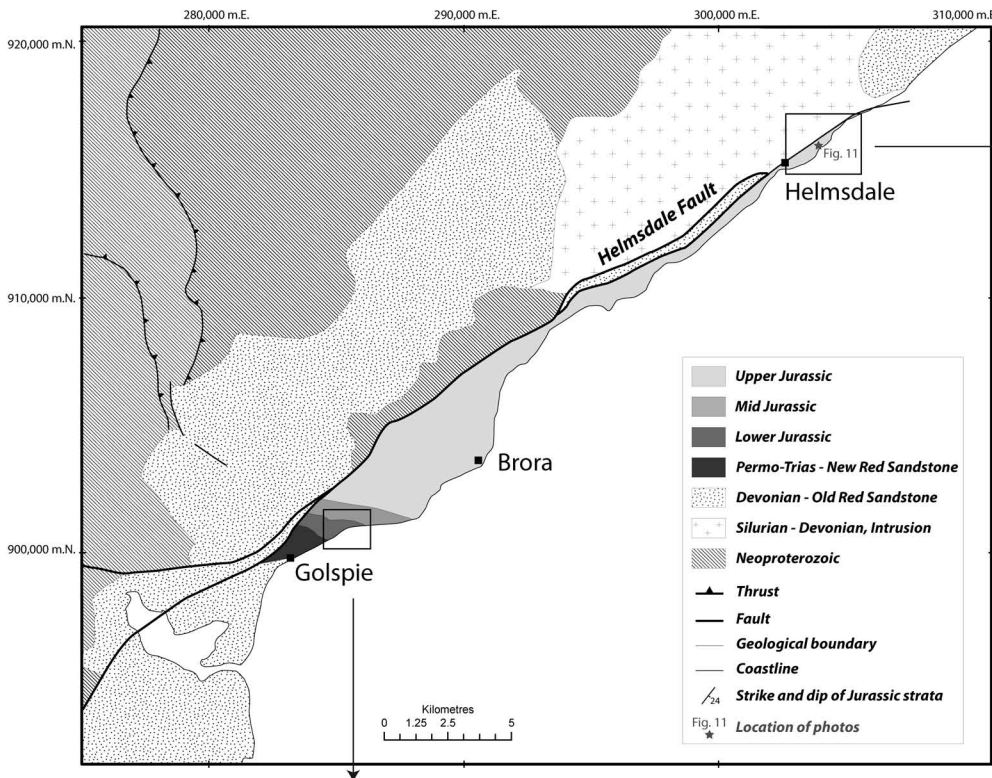
974,000 m.N.

973,000 m.N.

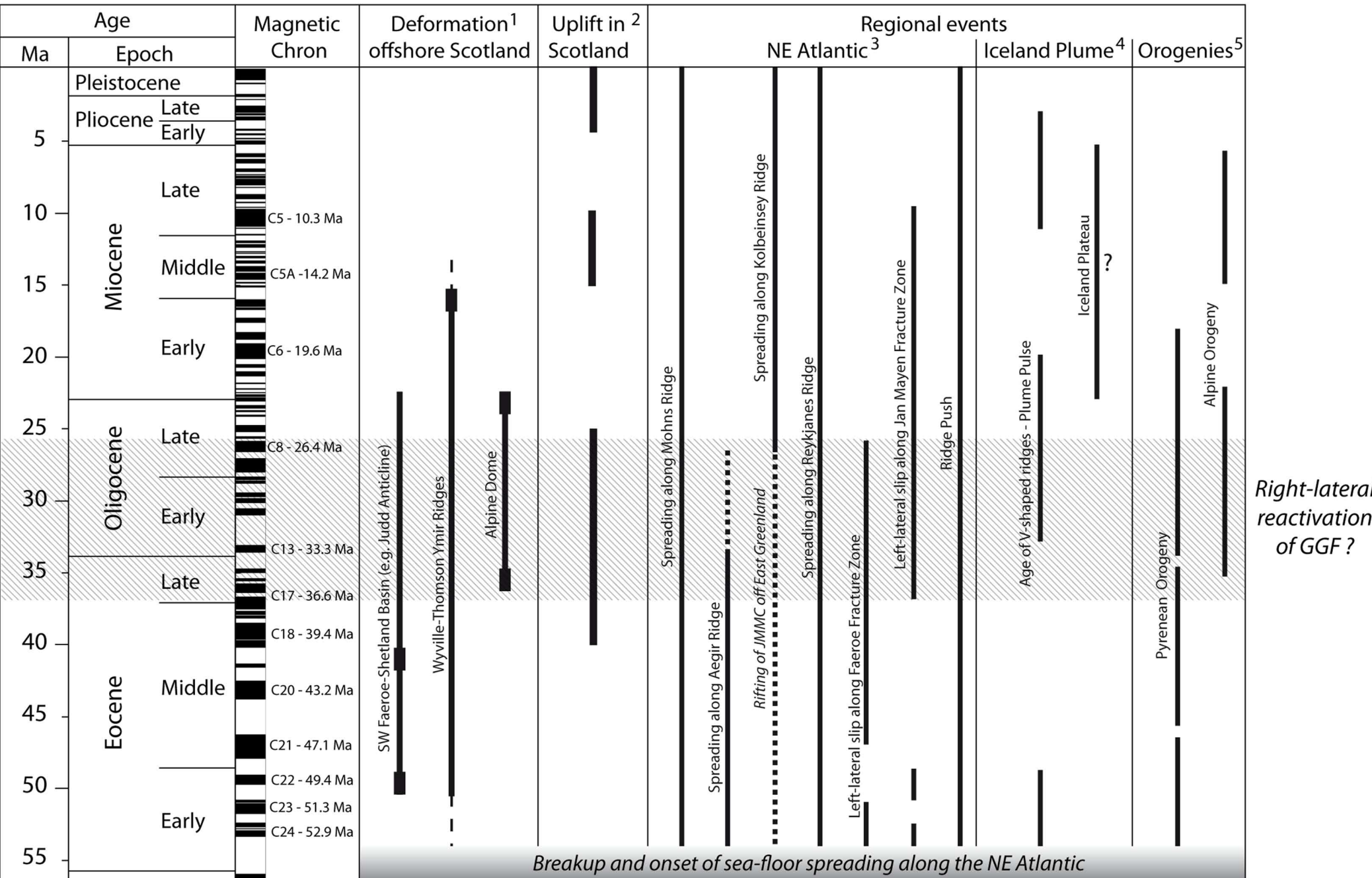




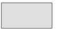

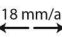













Chron 17 -36.6 Ma Late Eocene

-  Continent
-  COB Continent-Ocean Boundary
-  18 mm/a Direction and Rate of Spreading
-  Fracture Zone
- GFZ Greenland Fracture Zone
- SFZ Senja Fracture Zone
- CGFZ Charlie Gibbs Fracture Zone
- JMFZ Jan Mayen Fracture Zone
- FFZ Faeroe Fracture Zone
- JMMC Jan Mayen Microcontinent
- GGF** **Great Glen Fault**
- MTF** **Møre Trøndelag Fault**
-  Strike-Slip Motion along Fracture Zones
-  Principal Direction of Shortening
-  Rotations of JMMC and eastern side of Aegir Ridge
-  Post-breakup inversion structures

